ApJ, in press
Preprint typeset using LaTeX style emulateapj v. 04/03/99

SIMULATIONS OF ACCRETION FLOWS CROSSING THE LAST STABLE ORBIT

Philip J. Armitage[1,2]
Max-Planck-Institut für Astrophysik, Karl-Schwarzschild-Str. 1,
D-85741 Garching, Germany
pja3@st-andrews.ac.uk
Christopher S. Reynolds[3] and James Chiang
JILA, Campus Box 440, University of Colorado, Boulder CO 80303, USA
chris@rocinante.colorado.edu; chiangj@rocinante.colorado.edu
ApJ, in press

ABSTRACT

We use three dimensional magnetohydrodynamic simulations, in a pseudo-Newtonian potential, to study geometrically thin accretion disc flows crossing $r_{\rm ms}$, the marginally stable circular orbit around black holes. We concentrate on vertically unstratified and isothermal disk models, but also consider a model that includes stratification. In all cases, we find that the sonic point lies just inside $r_{\rm ms}$, with a modest increase in the importance of magnetic field energy, relative to the thermal energy, observed inside the last stable orbit. The time-averaged gradient of the specific angular momentum of the flow, (dl/dr), is close to zero within $r_{\rm ms}$, despite the presence of large fluctuations and continuing magnetic stress in the plunging region. The result that the specific angular momentum is constant within $r_{\rm ms}$ is in general agreement with traditional disk models computed using a zero-torque boundary condition at the last stable orbit.
Subject headings: accretion, accretion disks – black hole physics – MHD – stars: neutron – hydrodynamics – instabilities

1. INTRODUCTION

The existence of a marginally stable orbit is a distinctive feature of accretion flows onto black holes. Within $r_{\rm ms}$, stable circular orbits do not exist, and gas inevitably plunges on a short timescale into the hole. The location of the marginally stable orbit, which lies at $r_{\rm ms} = 6GM/c^2$ for a non-rotating hole, varies strongly with the spin parameter a for Kerr black holes. This variation, together with the assumption of a large change in the emission properties of the gas interior and exterior to $r_{\rm ms}$, is central to all attempts to measure a from observable quantities for both galactic (Zhang, Cui & Chen 1997) and supermassive black holes (Iwasawa et al. 1996; Dabrowski et al. 1997; Bromley, Chen & Miller 1997). Neutron stars, if they are sufficiently compact, could also possess a last stable orbit, though we will not consider this possibility further here.

The presence of gas on plunging orbits within $r_{\rm ms}$ can have observable consequences. It potentially modifies the profile of the relativistic iron Kα line that has been observed in the X-ray spectra of some Seyfert galaxies (Tanaka et al. 1995; Reynolds & Begelman 1997; Young, Ross & Fabian 1998), and may create detectable absorption signatures (Nandra et al. 1999). However, it has generally been believed that gas within $r_{\rm ms}$ does not have any *dynamical* importance, since the infall rapidly becomes supersonic a short distance inside the marginally stable orbit. Whatever complexities may develop in the flow subsequently are then causally disconnected from the disk at larger radius. This line of reasoning suggests that for modelling the disk (by which we mean the region of the flow outside the last stable orbit), it suffices to impose a zero-torque boundary condition at $r_{\rm ms}$ and ignore the interior region altogether. For the details of disk models constructed in this manner, we refer the reader to Abramowicz & Kato (1989), and references therein.

This simple hydrodynamic picture would be oversimplified if magnetic fields inside $r_{\rm ms}$ were strong enough to maintain a connection between the plunging region and the disk. A recent analysis by Krolik (1999) showed that if magnetic fields, generated in the disk, remain frozen into the gas as it inspirals within $r_{\rm ms}$, then the energy density in the fields can become comparable to the rest-mass energy density of the flow. Related ideas have also been proposed by Gammie (1999). In addition to altering the zero-torque boundary condition for the disk, the presence of extremely strong fields in the plunging region could have several potentially observable consequences (Agol & Krolik 2000). For example, the radiative efficiency of the disk, $\epsilon = L/\dot{M}c^2$, could be substantially increased. The analysis of Krolik (1999), however, depends upon a split of the accretion flow into two distinct regions, a disk at $r > r_{\rm ms}$ in which magnetic dynamo processes (Balbus & Hawley 1991; Brandenburg et al. 1995; Stone et al. 1996; for a review see e.g. Hawley & Balbus 1999) maintain a turbulent state, and a plunging region at $r < r_{\rm ms}$ in which it is assumed that magnetic flux is frozen into the fluid. This split is clearly an approximation, because the same turbulent processes that act to generate and destroy magnetic fields in the disk itself will continue to operate until some finite distance inside the last stable orbit. This may alter the conclusion that a rapid growth in the relative importance of magnetic fields is inevitable. The analytic

[1]CITA, University of Toronto, McLennan Labs, 60 St George Street, Toronto, Ontario M5S 3H8, Canada
[2]Present address: School of Physics and Astronomy, University of St Andrews, North Haugh, St Andrews, Fife, KY16 9SS, UK
[3]Hubble Fellow

analysis further assumes that the flow is axisymmetric and steady-state. This is also only approximately the case in a turbulent accretion flow, and needs to be tested via numerical simulations.

In this paper, we employ three dimensional magnetohydrodynamic (MHD) simulations to study the properties of the accretion flow as it crosses $r_{\rm ms}$. A pseudo-Newtonian potential appropriate for a non-rotating black hole (Paczynski & Wiita 1980) is used to mimic the relativistic effect of a last stable orbit within a non-relativistic MHD code. Within this approximation, simulating the evolution of magnetic fields within the plunging region is, if anything, expected to be easier than following the development of turbulence in the disk at larger radii. Within the disk, orbits are stable, and thus in the absence of turbulence a field loop in the plane of the disk will *always* be sheared out in azimuth until numerical reconnection sets in at the grid scale. Once into the plunging region there is only a finite (but large) amount of shear before the infalling gas reaches the black hole.

The accretion flow within $r_{\rm ms}$ has already been studied by Hawley (2000), who presented global MHD simulations of accretion tori with a geometry similar to that of popular ADAF (Narayan & Yi 1994) and ADIOS (Blandford & Begelman 1999) models for radiatively inefficient flows. This geometry is thought to be appropriate at relatively low accretion rates for both supermassive and stellar mass black hole systems (for observational support see, e.g., Gilfanov, Churazov & Revnivtsev 1999). The specific model considered was geometrically fairly thick at large radius ($r \gg r_{\rm ms}$), although near the last stable orbit the importance of pressure forces, and the vertical scale height, was smaller. Indeed, at $r = r_{\rm ms}$, the relative scale height was $(h/r) \sim 0.1$, which is similar to the value used in our simulations. Significant magnetic stresses within $r_{\rm ms}$ were obtained in these simulations, and in subsequent higher resolution simulations of the same geometry (Hawley & Krolik 2000).

Existing work suggests that the conditions at $r_{\rm ms}$ may differ for geometrically thin and thick disks (Popham & Gammie 1998). We therefore emphasize that in this paper we address only the case of geometrically thin disks. The existence of a thin disc implies that radiative cooling must be efficient, and this allows us to further simplify the problem by adopting an isothermal equation of state in lieu of solving the energy equation. Thin disks are the expected mode of accretion at high $\dot{M}$ in both Active Galactic Nuclei, and in stellar mass Galactic black hole sources.

2. NUMERICAL METHODS

2.1. *The ZEUS hydrodynamics code*

We simulate the accretion flow using the ZEUS code (Stone & Norman 1992a,1992b; Clarke, Norman & Fielder 1994; Norman 2000) to solve the equations of ideal magnetohydrodynamics. ZEUS is an explicit Eulerian finite difference code, formally of second order accuracy, which uses an artificial viscosity to reproduce shocks. Advantages of the code for accretion disk applications include a flexible choice of gridding and co-ordinate systems, and algorithms (Norman, Wilson & Barton 1980) that minimise spurious diffusion of angular momentum relative to mass.

The analyis of the behavior of magnetic fields in the plunging region by Krolik (1999) is independent of the existence of vertical stratification in the disk. For our initial simulations we therefore adopt the computationally easiest option, and consider a vertically unstratified disk (i.e. one where the vertical component of gravity is artificially set to zero), and an isothermal fluid, where the presure P is given by,

$$P = \rho c_s^2, \tag{1}$$

where c_s is the sound speed and ρ is the density. For our standard model we choose c_s such that the ratio of the sound speed to the circular orbital velocity at the last stable orbit, $c_s/v_\phi = 0.08$. In an unstratified simulation, of course, c_s plays no role in setting the vertical scale height of the flow. However, the ratio c_s/v_ϕ, which in a real disk is related to the relative disk scale height via $h/r \simeq c_s/v_\phi$, still determines the importance of radial pressure forces for the disk structure. The simulated flows are 'thin' in the sense that radial pressure forces, which scale as $(h/r)^2$, are small compared to the gravitational force. A model with smaller sound speed was also investigated. For better comparison with the simulations of Hawley (2000), we also ran a variant including the effect of vertical stratification.

Standard choices for the Courant number, $C_0 = 0.5$, and coefficient of artificial viscosity, $C_2 = 2.0$, were used throughout. Second order advection was used for all quantities. The only code scaling which needs to be mentioned is that for time. We adopt units in which the orbital period at $r_{\rm ms}$, $P_{\rm ms} = 7.7$.

2.2. *Paczynski-Wiita potential*

ZEUS is a Newtonian fluid dynamics code which does not model any of the effects of special or general relativity. Within this framework, we use a pseudo-Newtonian gravitational potential (Paczynski & Wiita 1980),

$$\psi = -\frac{GM}{r - r_g} \tag{2}$$

where $r_g = 2GM/c^2$, to model what is expected to be the dominant relativistic effect around a non-rotating black hole – the existence of an innermost stable orbit at $r_{\rm ms} = 6GM/c^2$.

2.3. *Initial and boundary conditions*

We simulate a wedge of the disk extending 30° in azimuth in cylindrical polar geometry, (r, z, ϕ). This limitation on the azimuthal extent of the domain has the undesirable effect of eliminating larger scale azimuthal modes of the magnetic field, which contribute significantly to the total power in global disk simulations (e.g. Armitage 1998). The local properties of disk turbulence (for example the relative strengths of radial and azimuthal field components), however, which are probably of more importance for this problem, are less affected by the size of the azimuthal domain.

The boundary conditions are periodic in ϕ, and set to outflow at both $r_{\rm min}$ and $r_{\rm max}$. Outflow boundary conditions are implemented in ZEUS by setting zero gradients for all flow variables at the boundary. We note that this choice of boundary conditions allows a significant toroidal magnetic field to be advected across the inner boundary – we have not attempted to impose Newtonian analogs of the general relativistic boundary conditions for magnetic fields at the event horizon of the black hole. From a numerical standpoint, the use of outflow boundary conditions is desirable to ensure that the simulations do indeed model magnetic instabilities, rather than purely hydrodynamic instabilities to which relatively narrow annuli, with reflecting boundaries, are known to be susceptible (e.g. Narayan & Goodman 1989). We use a uniform grid in both ϕ and z. In the radial direction, a uniform grid interior to $r_{\rm ms}$ is matched smoothly onto a grid at larger radii for which $\Delta r_{i+1} = k \Delta r_i$, with $k > 1$ a constant. This concentrates resolution in the region of greatest interest near, and within, the marginally stable orbit.

The initial conditions for the calculation are intended as thin disk analogs of the toroidal configuration used by Hawley (2000), with the additional assumption of isothermality. We take a gaussian surface density profile, centered at $r = 2r_{\rm ms}$, with an azimuthal velocity appropriate to Keplerian rotation. We relax this profile in a preliminary non-magnetic one dimensional calculation, to ensure that it is an accurate numerical equilibrium state. The resulting profile of ρ and v_ϕ is then mapped into three dimensions, and a seed magnetic field added. To evaluate the sensitivity of the results to the boundary conditions, three unstratified simulations were run, with different choices of seed field and associated boundary conditions in z. Two simulations were run with an initially vertical field imposed at all radii where the surface density exceeded a threshold value, taken to be approximately a quarter of the maximum value of the surface density. Periodic boundary conditions for all variables were imposed in the z direction. For the first simulation (the 'standard' run) the radial and vertical boundaries were at $r_{\rm min} = 1$, $r_{\rm max} = 5$, and $z = \pm 0.3$, in code units where $r_{\rm ms} = 1.5$. The initial field strength (in regions seeded with field) was such that the ratio of gas pressure to magnetic pressure, $\beta_z = 5000$. The numerical resolution was $n_r = 150$, $n_z = 32$ and $n_\phi = 40$ grid points, with 30 of the radial grid points interior to $r_{\rm ms}$. The second run simulated a cooler disk (with a sound speed half the previous value), in a larger computational volume, bounded by $1 < r < 10$ and $z = \pm 0.25$. This run used $n_r = 210$, $n_z = 32$ and $n_\phi = 48$ grid points, and an initial seed field $\beta_z = 800$. Finally, a simulation was run with parameters similar to the first, except starting with an initially azimuthal field, with $\beta_\phi = 100$. For this simulation the vertical boundary conditions were chosen to be reflecting, with the vertical components of both the velocity and the magnetic field set to zero on the boundaries. The resolution for this run was $120 \times 32 \times 40$ grid points.

Simulations that include vertical stratification are obviously more realistic, but they are also more demanding of computational resources, because the development of magnetically dominated low density regions at high $|z|$ places severe restrictions on the timestep. Numerical tricks can be used to mitigate this problem (Miller & Stone 2000), but for this paper we adopted the simpler approach of considering a volume containing only a small number of disk scale heights. We therefore reran the standard model, including the vertical component of gravity, in a domain bounded by $z = \pm 0.5$. This admits only a couple of scale heights at $r_{\rm ms}$. As in the standard model, periodic boundary conditions were used for the magnetic field in the vertical direction. For this run we used $n_r = 150$, $n_z = 48$ and $n_\phi = 40$ grid points.

It is worth noting at the outset that these simulations are not, and are not intended to be, realizations of the same physical situation, and thus the results will differ between them. An initially vertical field gives the fastest possible growth rate of the Balbus-Hawley (1991) instability. Additionally, a non-zero vertical flux boosts the strength of MHD turbulence and increases the effective Shakura-Sunyaev (1973) α parameter obtained (Hawley, Gammie & Balbus 1995). Substantially longer timescales are required to reach saturation with an initially azimuthal field. We have run both simulations that used the smaller computational domain until a significant fraction (around a half) of the initial mass had been accreted, and compare the results at this late stage when the flow in the inner regions of the disk, near $r_{\rm ms}$, has reached an approximate steady state.

3. RESULTS

Fig. 1 shows the growth in the magnetic energy of the radial magnetic field component in the standard unstratified model with an initially vertical (z direction, $\beta_z = 5000$) magnetic field. Around 10 orbits of evolution are required to reach a nonlinear state in the inner regions of the flow, during which time the radial magnetic field energy grows exponentially. The growth rate is consistent with the expected growth rate of the Balbus-Hawley instability in this field geometry (Balbus & Hawley 1991), evaluated at the smallest radius that has been seeded with magnetic field. Subsequent to the instabilities saturating, the field energy fluctuates but remains roughly constant, before finally starting to decline as a significant fraction of the disk is accreted. At the point the run was stopped, at $t = 200$, 65% of the initial mass had been accreted. The magnetic field was dominated by the toroidal component, with the ratio of magnetic field energy in the z, r and ϕ fields being approximately 1:2:30.

The simulation seeded with an azimuthal magnetic field shows similar behavior, but with much slower growth of the magnetic field energy, despite the initially higher ratio of the magnetic energy to the thermal energy. This configuration was run up to $t = 600$, by which time just under 40% of the initial disk mass had been accreted.

Fig. 2 shows the evolution of the disk surface density with time, for the standard run with an initial vertical field. The evolution differs somewhat from the standard diffusive evolution of a viscous annulus (e.g. Pringle 1981), due to both the varying amount of time required before the disk at different radii becomes fully turbulent, and due to the development of supersonic infall interior to $r_{\rm ms}$. However the general trend towards a broadening surface density profile, that remains relatively smooth, is recovered. Spatial fluctuations in Σ, shown in Fig. 3, are strongly sheared and thus predominantly azimuthal in extent. When normalised to the mean surface density as a function of radius, as in the figure, there is no obvious visual indication of the location of the marginally stable orbit.

The radial and azimuthal velocities as a function of radius obtained in the standard run are shown in Fig. 4. A small radial velocity within the disk itself transitions smoothly into rapid infall within the marginally stable orbit. The sonic point lies somewhat inside $r_{\rm ms}$ (within a radial distance $\sim h$, the disk scale height that would correspond to the assumed sound speed). Note that the radial velocity slightly *outside* the marginally stable orbit is already beginning to increase in magnitude, in advance of reaching the actual infall region. Beyond $r \approx 2r_{\rm ms}$, the radial velocity is *outward*. This is a consequence of the initial surface density profile and the use of a free outer boundary condition. We have also experimented with runs in which mass was continually injected across the outer boundary, and the disk allowed to evolve until a quasi-steady state was achieved. These runs yielded similar results to those reported here – in particular there was no strong amplification of magnetic field observed interior to $r_{\rm ms}$. However, with inflow boundary conditions at $r_{\rm out}$ it is hard to be sure that purely hydrodynamic instabilities, which are known to occur within relatively narrow annuli when the boundary conditions are reflecting, do not contaminate the results. We therefore concentrate attention on the current simulations which follow a ring of gas which is allowed both to accrete and to spread to larger radii.

As expected for a thin disk, in which radial pressure forces are small compared to the gravitational force, the azimuthal velocity in the disk, v_ϕ, is very close to the Keplerian value for orbits in a Paczynski-Witta potential.

The presence of magnetic fields in the flow potentially allows the flow interior to the sonic point to communicate with the exterior disk. Generically, except in unusual circumstances, MHD turbulence driven by the Balbus-Hawley instability saturates at a level where the magnetic pressure in the disk is substantially less than the thermal pressure, typically by one or two orders of magnitude (Hawley, Gammie & Balbus 1995; Brandenburg et al. 1995; Stone et al. 1996). Stronger fields, relative to the gas pressure, are likely to occur in the disk corona (Miller & Stone 2000). As shown in Fig. 5 for our standard unstratified simulation, the mean Alfven speed in the disk, $v_A = \sqrt{(B^2/4\pi\rho)}$, remains less than the sound speed at all radii. This is even more true for the simulation with the initial ϕ field, not shown in the figure, since the saturation level of the magnetic fields in that run is significantly below the value obtained in the initial vertical field runs. Similarly, for the vertically stratified version of the standard run, the mean Alfven speed is smaller than the sound speed at all radii, and is of similar magnitude to the unstratified case. For this run, the magnetic fields and the Alfven speed near the disk midplane, also plotted in Fig. 5, are significantly greater than the mean value in the plunging region, though not by a large factor.

These results do not, however, exclude the possibility that the plunging region can exert a torque on the disk at the last stable orbit. In the presence of turbulence, some regions of the flow have relatively stronger magnetic fields (or lower density), with correspondingly higher Alfven speed. As a result, the critical point can penetrate further into the plunging region than one would estimate based solely on the mean flow properties. As shown in Fig. 5, for both the stratified and the unstratifed runs, we find that the *peak* Alfven speed at any radius is substantially greater than the mean value. Although it does not rise as rapidly as the absolute value of the radial velocity, it is therefore possible, at least in principle, for the plunging region some distance inside the last stable orbit to be in communication with the disk at larger radii. In our simulations this distance is still only $\sim h$, but whether this result also holds for cooler flows is currently unknown.

Fig. 6 shows the ratio of the magnetic energy to the thermal energy for the standard run, and for the run with an initially azimuthal seed magnetic field, as a function of radius. A single timeslice from the simulation produces a rather noisy estimate of this quantity, so we plot the average from 5 independent epochs close to the end of the run ($t = 150$ to $t = 200$ for the z field run, and $t = 440$ to $t = 600$ for the ϕ field case). The ratio $(B^2/8\pi\rho c_s^2)$ is around 0.05 - 0.1 for the initial z field run with $\beta_z = 5000$, and is modestly greater for the run using a larger computational domain and an initial $\beta_z = 800$. These values are consistent with the values (0.1 - 0.2) obtained by Hawley, Gammie & Balbus (1995) from unstratified local simulations in the shearing-box geometry, at comparable initial $\beta_z = 3200$. As expected, the fields are significantly weaker in the simulation with an initial ϕ field and non-periodic boundary conditions in z. In this case we obtain a ratio of magnetic to thermal energy in the $1 - 2 \times 10^{-2}$ range. In all the runs, modest field amplification interior to the marginally stable orbit is observed. The fields remain well below equipartition with the thermal energy, while the kinetic energy is of course orders of magnitude greater still.

Angular momentum transport in the disk is dominated by magnetic, rather than fluid, stresses. We also plot in Fig. 6 a measure of the magnetic stress, normalised to the gas pressure,

$$\alpha_{\rm mag} = \frac{2}{3} \langle \frac{-B_r B_\phi}{4\pi\rho c_s^2} \rangle, \tag{3}$$

which in the disk is just the magnetic contribution to the Shakura-Sunyaev α parameter. Typical values obtained are a few $\times 10^{-2}$ for the standard simulation, and somewhat less than 10^{-2} for the simulation with an initial magnetic field in the ϕ direction. From the figure, it can also be seen that there is continuing magnetic stress, and a rise in $\alpha_{\rm mag}$, within the plunging region, where the density drops rapidly. In these plots there is evidently nothing special about the location $r = r_{\rm ms}$, and the magnetic torque does not vanish there. The existence of this stress inside $r_{\rm ms}$, which is one of the predictions of Krolik (1999), has also been seen in previous numerical simulations (Hawley 2000; Hawley & Krolik 2000).

For the vertically stratified run, we have also checked for the presence of significant variations of $\alpha_{\rm mag}$, and other quantities, with z. Interior to $r_{\rm ms}$, the strength of the magnetic stress, normalised to the gas pressure, is found to be greater near the midplane of the disk than at larger z, but only modestly so.

To test the effect of this ongoing stress on the dynamics of the flow inside the last stable orbit, we plot in Fig. 7 the specific angular momentum l of the flow as a function of radius. To reduce fluctuations in l, we average the specific angular momentum over several timeslices taken from near the end of the simulations. For all the runs, $l(r)$ in the disk ($r > r_{\rm ms}$) is close to the Keplerian value for circular orbits in the pseudo-Newtonian potential, apart from a deviation close to $r_{\rm ms}$ where the radial density gradient is becoming large. At a zero-torque boundary, we expect that dl/dr vanishes. There is some variation in l within the marginally stable orbit, even in the averaged profiles, and weak indications of a small systematic decline towards smaller radii. This is consistent with the aforementioned presence of magnetic stress inside $r_{\rm ms}$. However, it is clear from Fig. 7 that for both the unstratified and stratified simulations the specific angular momentum is close to flat within $r_{\rm ms}$. The magnetic stress that exists within $r_{\rm ms}$ does not appear to be sufficient to change l significantly within the last stable orbit. In this (restricted) sense, the numerical results are broadly consistent with the standard, purely hydrodynamic, picture of thin disk accretion accretion onto black holes (Abramowicz & Kato 1989), which assumes a zero-torque boundary condition at the last stable orbit.

The highest resolution of the runs discussed here is obtained in the vertically stratified simulation. For this run, we plot in Fig. 8 the specific angular momentum from 5 timeslices, evenly spaced between $t = 150$ and $t = 200$. Significant fluctuations in l at any given radius are present. The influence of such fluctuations on the average structure of the disk outside $r_{\rm ms}$ is unclear, though we speculate that they could lead to significant changes in, for example, the radiative efficiency of the flow. However, in none of the slices do we see evidence for the clear and continuing decline in l, interior to the marginally stable orbit, that was obtained in the simulations of Hawley (2000).

4. DISCUSSION

In this paper, we have used MHD simulations to study the transition between a geometrically thin accretion disk, in which inflow is driven by the rate at which turbulence can transport angular momentum outwards, and the unstable plunging region interior to the marginally stable orbit. We find that in many respects the transition resembles that expected on the basis of previous analytic and one-dimensional numerical calculations (Paczynski & Bisnovatyi-Kogan 1981; Muchotrzeb & Paczynski 1982; Muchotrzeb 1983; Matsumoto et. al. 1984; Abramowicz & Kato 1989). In particular, we find no evidence, at least in pseudo-Newtonian simulations at the current resolution, for the extremely strong growth in the importance of magnetic fields (relative to the thermal or rest-mass energy of the flow) and associated dynamical effects discussed by Krolik (1999). Indeed, in these thin disk simulations, the average specific angular momentum is close to flat at and within the last stable orbit. In this respect, the numerical results, at least for the time averaged state, appear to be consistent with disk models computed using a zero-torque boundary condition at the last stable orbit. This differs from the results of some previous simulations (Hawley 2000; Hawley & Krolik 2000), in which an unmistakeable decline in the specific angular momentum inside $r_{\rm ms}$ was obtained. Although the conditions at $r_{\rm ms}$ are expected to vary between thin and thick disks, the model computed by Hawley (2000) and Hawley & Krolik (2000) is thin enough at $r_{\rm ms}$ that $l(r)$ is close to Keplerian. We speculate that differences in the equation of state, spatial domain, or numerical resolution could be responsible for the discrepancy. Further simulations investigating these possibilities are in progress.

Although we have not found any strong dynamical effects associated with magnetic fields interior to the last stable orbit, we do see evidence for the essential ingredient – ongoing magnetic stresses in the plunging region – of recent models that have questioned the validity of a zero-torque boundary condition for black hole accretion (Gammie 1999; Krolik 1999; Agol & Krolik 2000). The differences between these simulations, and those presented by Hawley (2000) and Hawley & Krolik (2000), are thus quantitative rather than qualititive in nature. We would therefore emphasize that further improvements in the simulations are required to investigate the behavior of the vertically stratified flows more robustly, to extend the simulations to test the evolution of cooler flows crossing the last stable orbit, and to explore the continuum between geometrically thin and thick disks.

The simulations reported here are non-relativistic, and cannot – even crudely – be extended to model any of the additional complexity that arises if the accretion flow is onto a Kerr black hole. Considerable progress has been made in the development of numerical methods for general relativistic hydrodynamics and magnetohydrodynamics (e.g. Font 2000), but these methods are probably not yet able to follow a turbulent disk flow transiting the last stable orbit. We note, however, that the general relativistic MHD calculations that have already been reported do show important differences with non-relativistic analogs (Koide, Shibata & Kudoh 1999; Meier 1999; Koide et al. 2000), and this should be borne in mind as an important caveat to the results presented here. The dynamics of the inner disk could also be modified by magnetic fields exterior to the disk, either in a disk corona (Miller & Stone 2000; Hawley & Krolik 2000), or by fields linking the disk to a spinning black hole (Livio 1999; Blandford 1999). Given the diverse range of variability observed in accreting black hole systems, further exploration of such ideas is clearly warranted.

We thank the developers of ZEUS and ZEUS-MP for making these codes available as community resources through the Laboratory for Computational Astrophysics, and Charles Gammie, Julian Krolik and Bohdan Paczynski for valuable comments. CSR acknowledges support from Hubble Fellowship grant HF-01113.01-98A. This grant was awarded by the Space Telescope Institute, which is operated by the Association of Universities for Research in Astronomy, Inc., for NASA under contract NAS 5-26555. CSR also thanks support from the NSF under grants AST 9876887 and AST 9529170. JC was supported by NASA/ATP grant NAGS5-7723.

REFERENCES

Abramowicz, M.A., Kato, S., 1989, ApJ, 336, 304
Agol E., Krolik J.H., 2000, ApJ, 528, 161
Armitage P.J., 1998, ApJ, 501, L189
Balbus S.A., Hawley J.F., 1991, ApJ, 376, 214
Blandford, R.D., 1999, in Astrophysical Disks, eds. Sellwood & Goodman, ASP Conf. Series, 160, p. 265
Blandford, R.D., Begelman, M.C., 1999, MNRAS, 303, 1
Bromley, B.C, Chen, K., Miller, W.A., 1997, ApJ, 475, 57
Brandenburg A., Nordlund A., Stein R.F., Torkelsson U., 1995, ApJ, 446, 741
Clarke D.A., Norman M.L., Fiedler R.A., 1994, National Center for Supercomputing Applications Technical Report 15

Dabrowski, Y., Fabian, A.C., Iwasawa, K., Lasenby, A.N., Reynolds, C.S., 1997, MNRAS, 288, 11
Font, J.A., 2000, Living Reviews in Relativity, 3, 2000-2, gr-qc/0003101
Gammie C.F., 1999, ApJ, 522, L57
Gilfanov, M., Churazov, E., Revnivtsev, M., 1999, A&A, 352, 182
Hawley, J.F., 2000, ApJ, 528, 462
Hawley J.F., Balbus S.A., 1999, in Astrophysical Disks, eds. Sellwood & Goodman, ASP Conf. Series, 160, p. 108
Hawley, J.F., Gammie, C.A., Balbus, S.A., 1995, ApJ, 440, 742
Hawley, J.F., Krolik, J.H., 2000, ApJ, in press, astro-ph/0006456
Iwasawa K. et al., 1996, MNRAS, 282, 1038
Koide, S., Meier , D.L., Shibata, K., Kudoh, T., 2000, ApJ, 536, 668
Koide, S., Shibata, K., Kudoh, T., 1999, ApJ, 522, 727
Krolik J.H., 1999, ApJ, 515, L73
Livio, M., 1999, in Astrophysical Disks, eds. Sellwood & Goodman, ASP Conf. Series, 160, p. 33
Matsumoto, R., Kato, S., Fukue, J., Okazaki, A.T., 1984, PASJ, 36, 71
Meier D.L., 1999, ApJ, 522, 753
Miller, K.A., Stone, J.M., 2000, ApJ, 534, 398
Muchotrzeb, B., 1983, Acta. Astron., 33, 79
Muchotrzeb, B., Paczynski, B., 1982, Acta. Astron., 32, 1
Nandra K., George I.M., Mushotzky R.F., Turner T.J., Yaqoob T., 1999, ApJ, 523, L17
Narayan R., Goodman J., 1989, in Theory of Accretion Disks, eds. F. Meyer, W.J. Duschl, J. Frank, E. Meyer-Hofmeister, Kluwer (Dordrecht), p. 231
Narayan, R., Yi, I., 1994, ApJ, 428, 13
Norman, M.L., 2000, in Astrophysical Plasmas: Codes, Models & Observations, eds J. Arthur, N. Brickhouse and J. Franco, Rev. Mex. Astron. Astrophys. (Conf. Ser.), 9, 66, astro-ph/0005109
Norman, M.L., Wilson, J.R., Barton, R., 1980, ApJ, 239, 968
Paczynski, B., Bisnovatyi-Kogan, G., 1981, Acta. Astron., 31, 283
Paczynski B., Wiita P.J., 1980, A&A, 88, 23
Popham, R., Gammie, C.F., 1998, ApJ, 504, 419
Pringle, J.E., 1981, ARA&A, 19, 137
Reynolds C.S., Begelman M.C., 1997, ApJ, 488, 109
Shakura N.I., Sunyaev R.A., 1973, A&A, 24, 337
Stone J.M., Hawley J.F., Gammie C.F., Balbus S.A., 1996, ApJ, 463, 656
Stone J.M., Norman M.L., 1992a, ApJS, 80, 791
Stone J.M., Norman M.L., 1992b, ApJS, 80, 819
Tanaka Y. et al., 1995, Nature, 375, 659
Young, A.J., Ross, R.R., Fabian, A.C., 1998, MNRAS, 300, 11
Zhang, S.N., Cui, W., Chen, W., 1997, ApJ, 482, L155

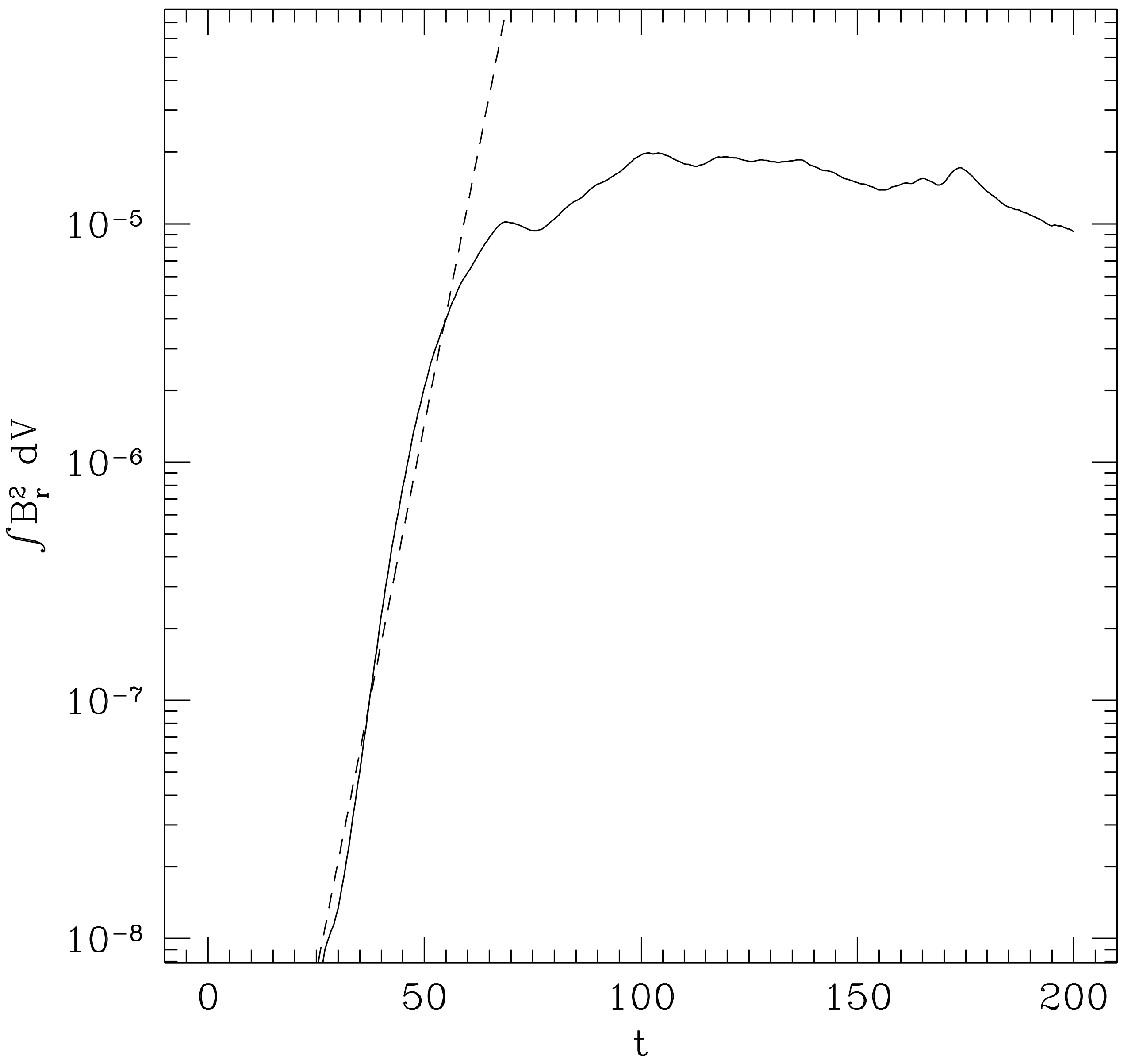

FIG. 1.— Energy in the radial component of the magnetic field, integrated over the simulation volume, as a function of time. The units on the vertical axis are arbitrary. The initial magnetic field for this simulation was in the z direction, and the vertical boundary conditions were periodic. The dashed line shows the expected growth rate of the radial magnetic field energy density, for the most unstable (largest Ω) mode.

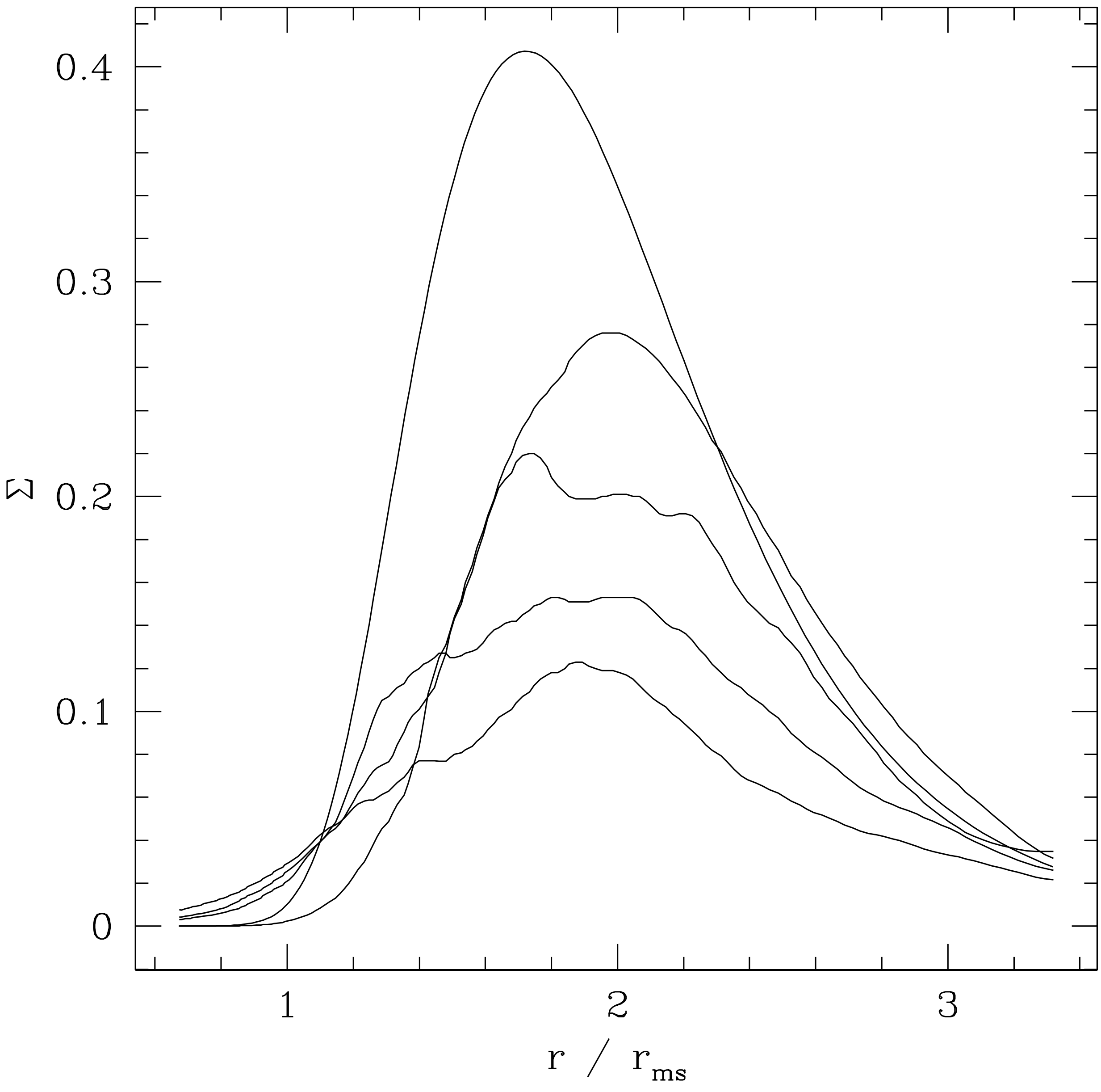

FIG. 2.— Evolution of the disk surface density profile in the simulation with an initially vertical magnetic field geometry. From top down, the slices are plotted at t = 0, t = 50, t = 100, t = 150, and t = 200. More than half of the mass has been accreted by the end of the simulation.

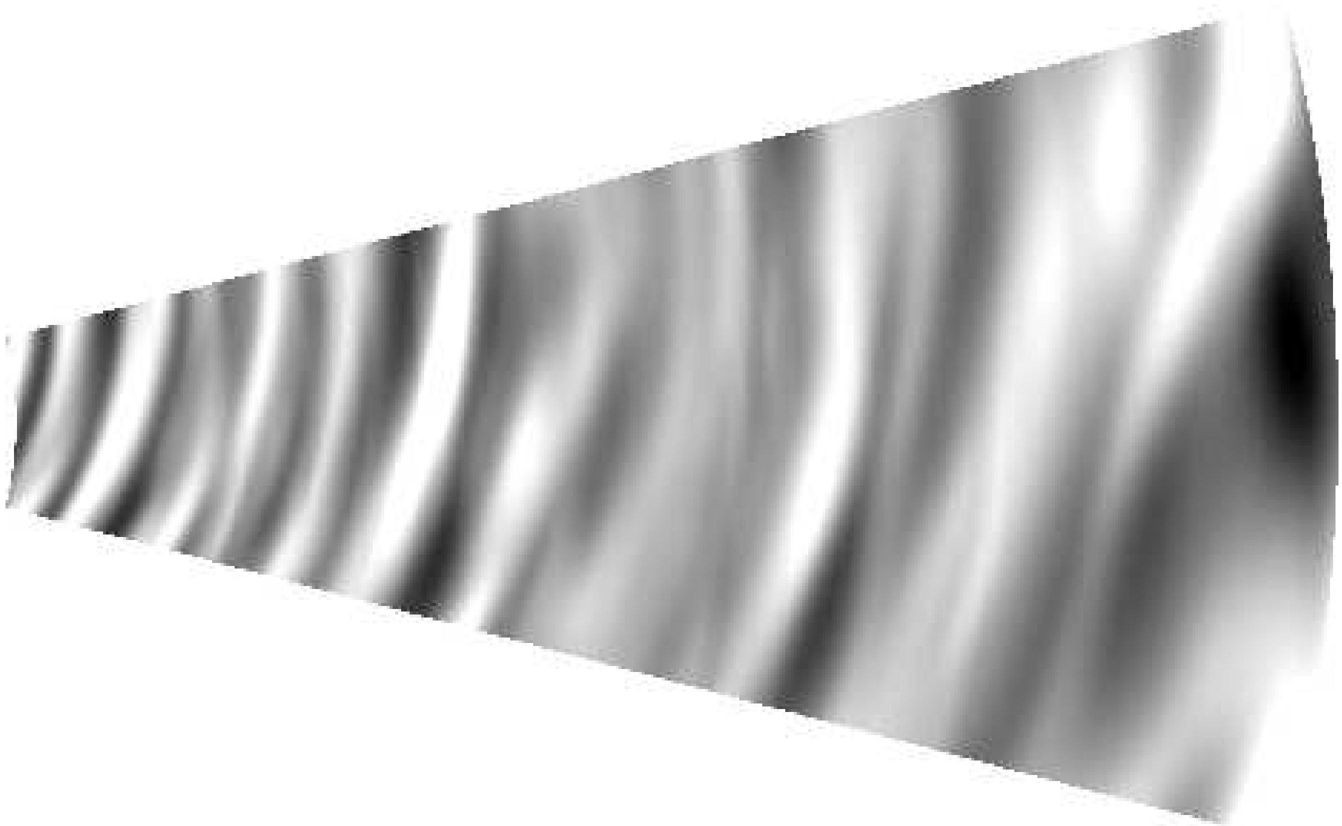

FIG. 3.— Image of the disk surface density fluctuations, $\Sigma(r,\phi)/\Sigma(r)$. The inner boundary is at 0.66 $r_{\rm ms}$, the outer boundary at 3.33 $r_{\rm ms}$. The magnitude of the fluctuations is at the $\sim 10\%$ level. No qualitative changes are noticeable as the flow crosses the marginally stable orbit.

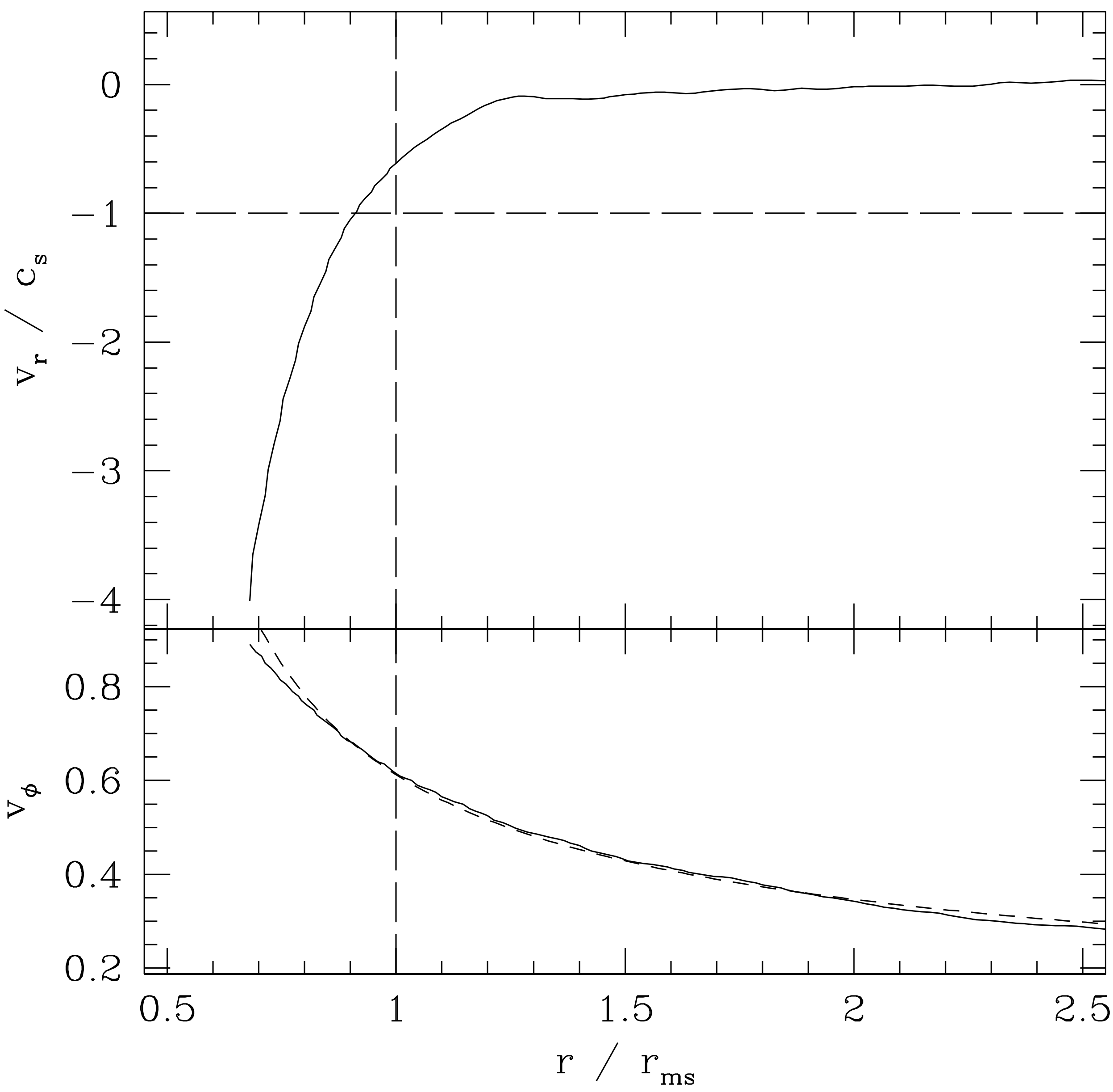

FIG. 4.— Radial and azimuthal velocity at t = 200 from the standard simulation. The short dashed curve in the lower panel shows the Keplerian velocity of circular orbits in the pseudo-Newtonian potential, in units where $c = 1$.

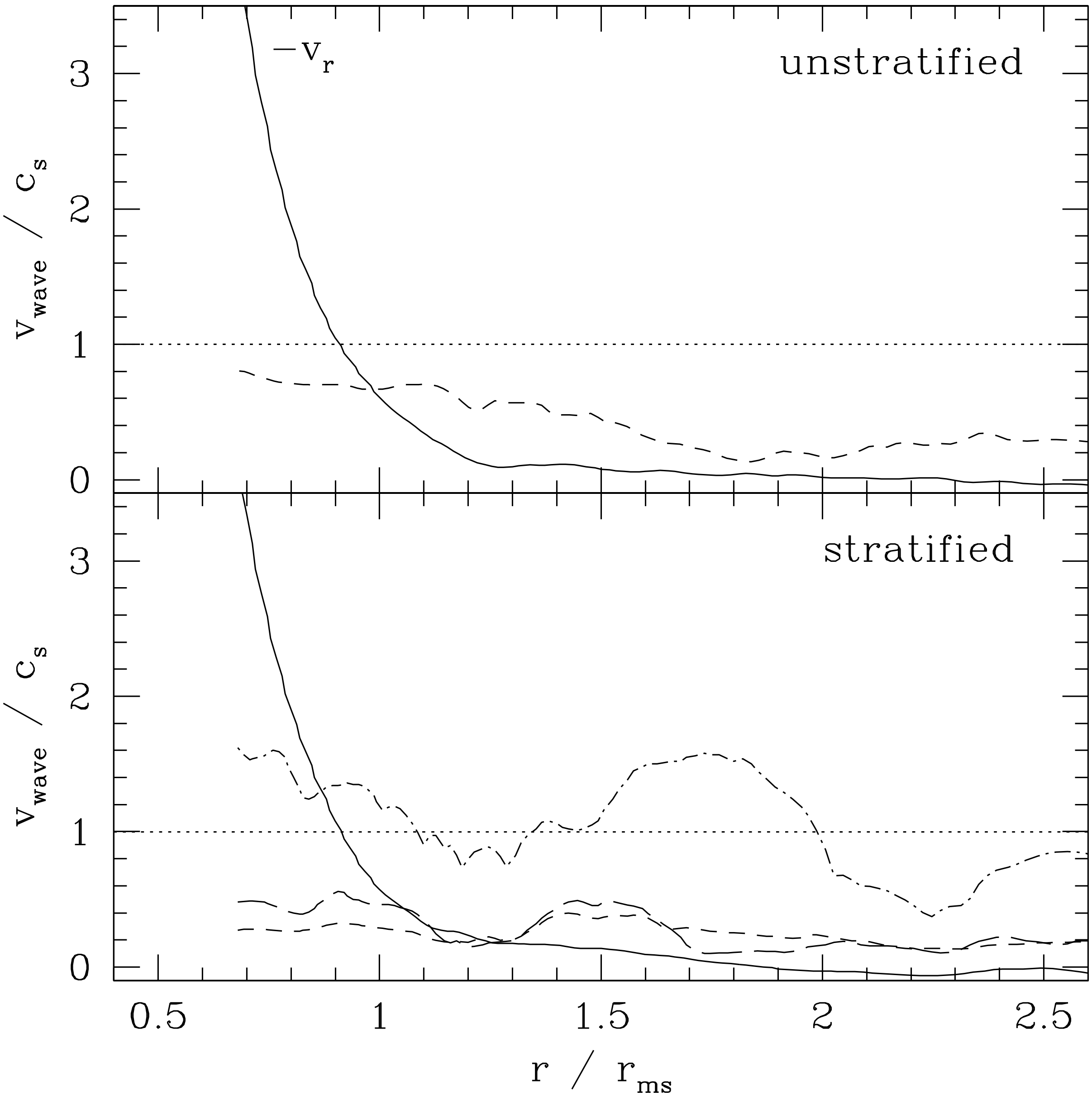

FIG. 5.— Wave propagation speed as a function of radius, evaluated at $t = 200$ from the standard simulation with and without vertical stratification. In the upper panel, for the unstratified run, the horizontal dotted line shows the sound speed, the short dashed line the mean Alfven speed as a function of radius. The negative of the radial velocity is plotted as the solid curve. The lower panel shows the same quantities plotted for the stratified simulation, with the long dashed line showing the mean Alfven speed in the flow near the disk midplane ($|z| < 0.1$). We also plot the *peak* Alfven speed at each radius (dot-dashed line), which exceeds the mean value by a substantial factor.

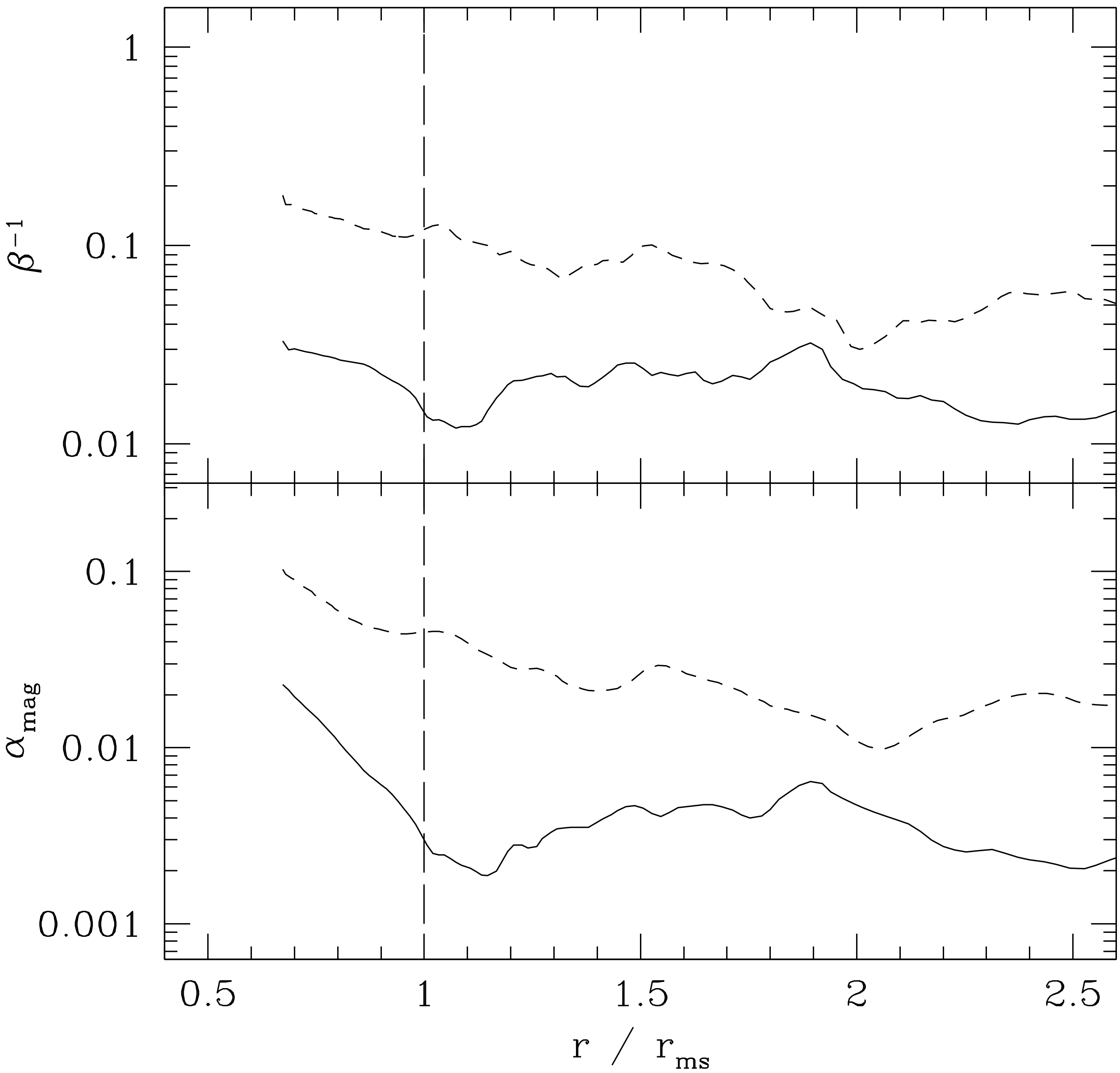

FIG. 6.— The upper panel shows the ratio of the magnetic energy to the thermal energy, as a function of radius, for the standard simulation with an initial z field (dashed line), and for the run with an initial ϕ field (solid line). In both cases, several timeslices from near the end of the runs have been averaged together to reduce the magnitude of the fluctuations. The lower panel shows the effective Shakura-Sunyaev α parameter derived from the magnetic torques.

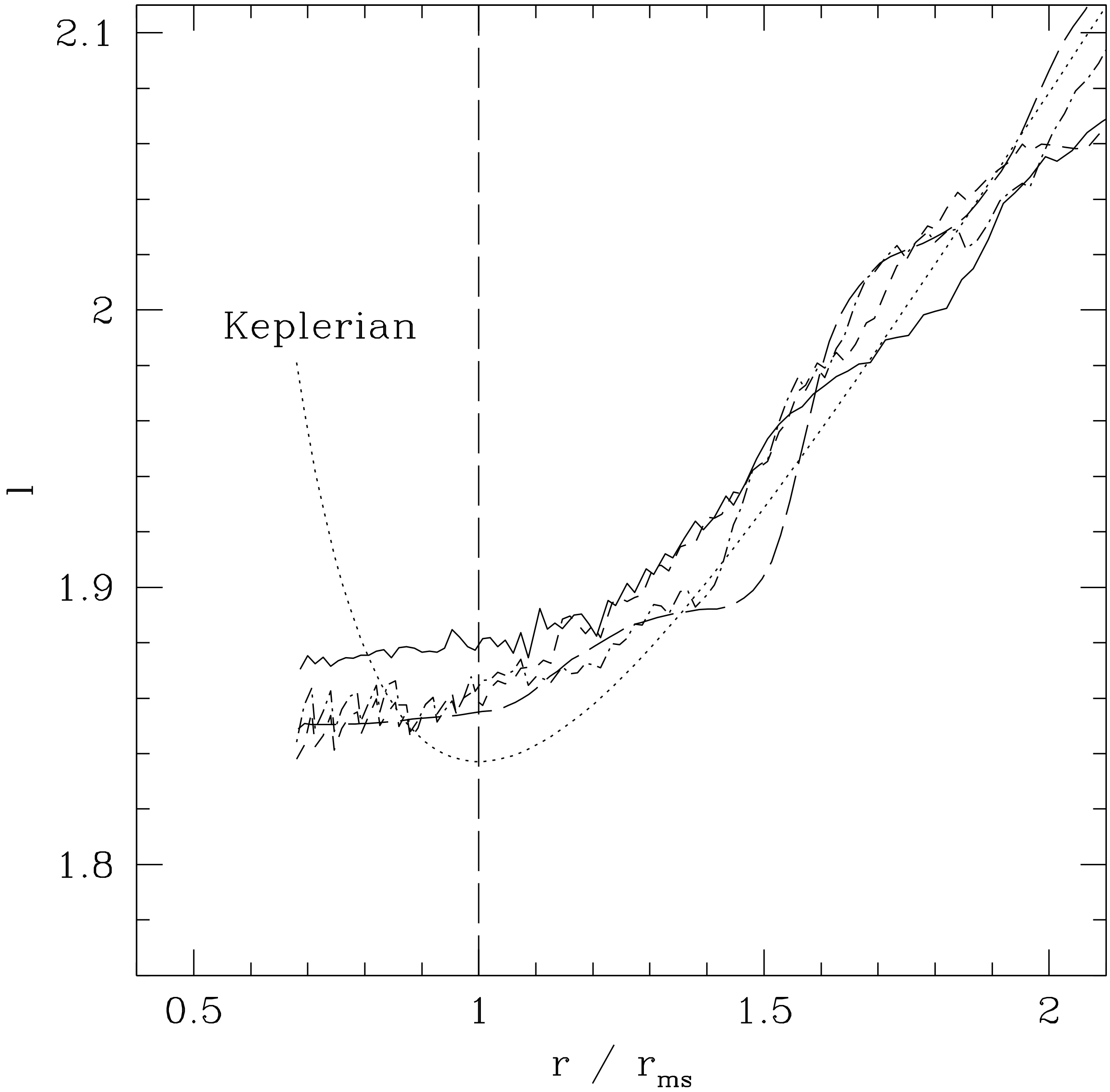

FIG. 7.— The specific angular momentum l as a function of radius. The solid line shows the result for the unstratified simulation with an initial ϕ magnetic field, the short dashed and long dashed curves for unstratified simulations with an initial z field but different sound speeds and seed field strength. The dot-dashed line shows the result for the vertically stratified simulation, evaluated in the disk midplane. Note that the simulation with reduced sound speed (long dashed line) evolves more slowly, so that the averaging of several timeslices has not eliminated substantial fluctuations present at larger radius outside r_{ms}. For all these models, dl/dr is close to zero at r_{ms}. The dotted curve shows the specific angular momentum of circular orbits in the pseudo-Newtonian potential.

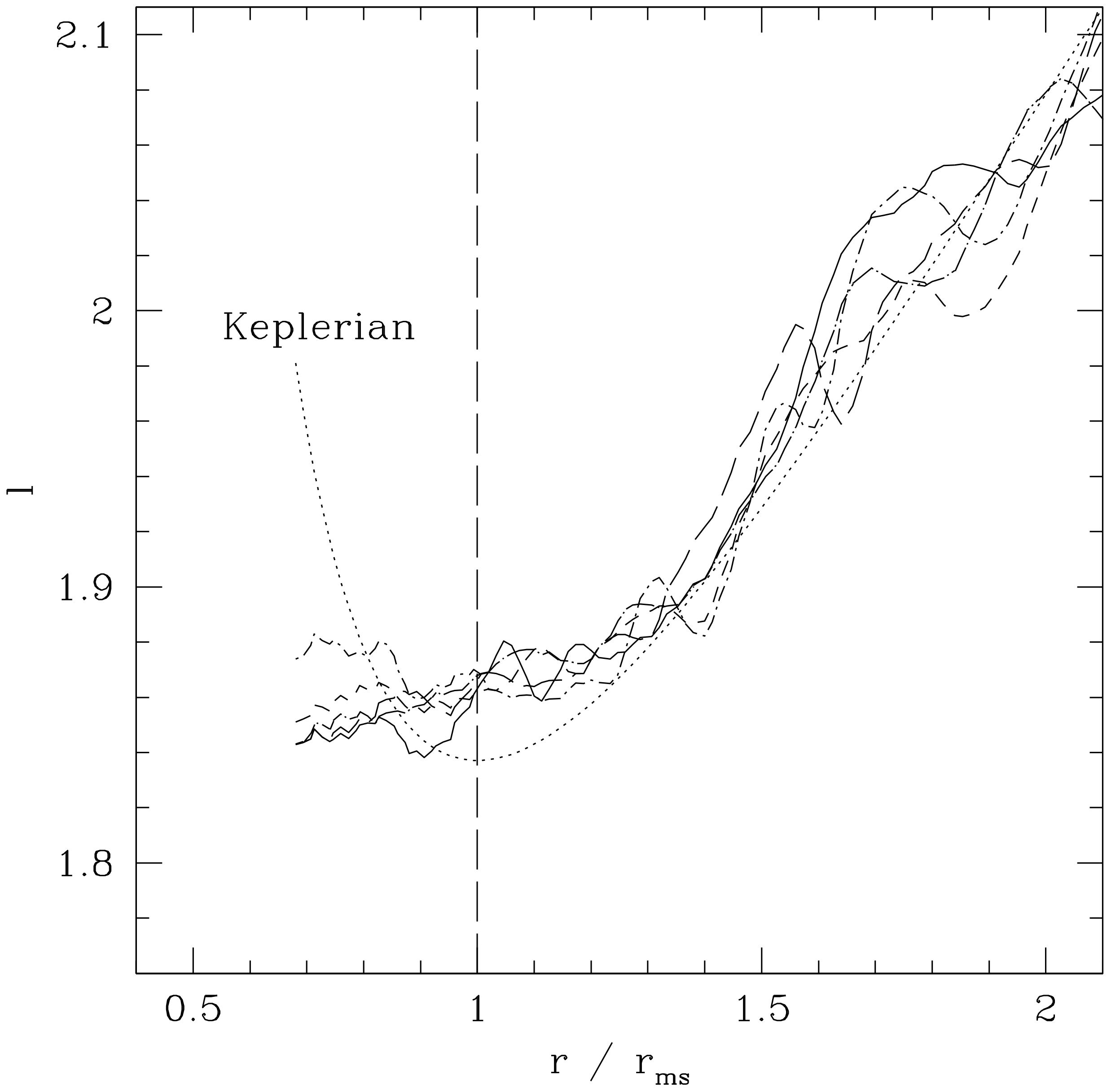

FIG. 8.— The specific angular momentum l as a function of radius, plotted from five timeslices of the stratified run. As in Fig. 7, l is evaluated in the disk midplane. The dotted curve shows the specific angular momentum of circular orbits in the pseudo-Newtonian potential.